

W^+W^- , WZ and ZZ production in the POWHEG BOX

Tom Melia

Rudolf Peierls Centre for Theoretical Physics, 1 Keble Road, University of Oxford, UK
E-mail: t.melia1@physics.ox.ac.uk

Paolo Nason

INFN, Sezione di Milano Bicocca, Italy
E-mail: Paolo.Nason@mib.infn.it

Raoul Röntsch

Rudolf Peierls Centre for Theoretical Physics, 1 Keble Road, University of Oxford, UK
E-mail: r.rontsch1@physics.ox.ac.uk

Giulia Zanderighi

Rudolf Peierls Centre for Theoretical Physics, 1 Keble Road, University of Oxford, UK
E-mail: g.zanderighi1@physics.ox.ac.uk

ABSTRACT: We present an implementation of the vector boson pair production processes ZZ , W^+W^- and WZ within the POWHEG framework, which is a method that allows the interfacing of NLO calculations to shower Monte Carlo programs. The implementation is built within the POWHEG BOX package. The Z/γ^* interference, as well as singly resonant contributions, are properly included. We also considered interference terms arising from identical leptons in the final state. As a result, all contributions leading to the desired four-lepton system have been included in the calculation, with the sole exception of the interference between ZZ and W^+W^- in the production of a pair of same-flavour, oppositely charged fermions and a pair of neutrinos, which we show to be fully negligible. Anomalous trilinear couplings can be also set in the program, and we give some examples of their effect at the LHC. We have made the relevant code available at the POWHEG BOX web site.

KEYWORDS: POWHEG, SMC, NLO, QCD.

Contents

1. Introduction	1
2. Description of the implementation	2
3. Results	4
3.1 ZZ Production	5
3.2 W^+W^-/WZ Production	10
4. Conclusion	14
A. Phase space sampling	15
B. Born zeros	16

1. Introduction

The pair production of electroweak vector bosons is of great interest to the particle physics community. The leptonic decay of electroweak boson pairs has been intensively studied at the Tevatron [1–9], while first measurements of W^+W^- production were recently published by both ATLAS [10] and CMS [11].

Vector boson pair production is interesting for various reasons. First of all, the process is interesting in itself, as a test of the non-Abelian nature of the electroweak force. Any deviation from the Standard Model tri-vector boson couplings would indicate the presence of new physics. Electroweak boson pair production is also an irreducible background to moderately heavy Higgs production, where the Higgs decays into electroweak bosons. It is therefore essential that we are able to make accurate predictions for these processes.

In general, calculations at leading-order (LO) in perturbative QCD (pQCD) have a large dependence on the unphysical factorization and renormalization scales. In order to limit these uncertainties, it is necessary to extend the pQCD calculations to next-to-leading order (NLO). Analytic formulae for the LO and NLO matrix elements for a weak boson pair decaying to leptons, written succinctly in the helicity formalism, were presented in ref. [12]¹. These have been implemented in publicly available programs, such as MCFM [14, 15], enabling fast computations for these processes.

However, the presence of soft and collinear divergences in the final state means that any computation performed at NLO can only provide accurate predictions for inclusive

¹Although $q\bar{q} \rightarrow W^+W^-$ with decays was previously considered to $\mathcal{O}(\alpha_s)$ in Ref. [13], the virtual correction to the spin correlations were not computed there.

quantities. On the other hand, exclusive quantities are often of great interest when analyzing an event - for example, any quantity including a jet variable in weak boson pair production. In order to compute exclusive quantities accurately, parton shower programs must be used. Two methods exist to interface NLO results to parton shower programs: **MC@NLO** [16] and **POWHEG** [17, 18]. In fact, W^+W^- -pair production was the first process studied in the former [16], while ZZ production was the first practical demonstration of the latter approach [19]. Furthermore, W^+W^- , $W^\pm Z$ and ZZ production have been studied within the **POWHEG** framework in refs. [20, 21]. Notwithstanding this, a full, public NLO implementation of electroweak boson pair production, including leptonic decays, Z/γ^* interference and non-resonant graphs, is still missing, and is badly needed by the experimental collaborations in order to reliably simulate their backgrounds away from the resonant region. The purpose of the present work is to fill this gap by providing NLO implementations for weak boson pair production that include all diagrams that lead to the desired 4-lepton final states. The only effect not included is the interference between the W^+W^- and ZZ pair production when the final state consists of two opposite charged leptons and a neutrino-antineutrino pair of the same family. We show, however, that this effect is fully negligible.

A formally NNLO contribution to these processes, initiated by gluon fusion, is also known to be important. We do not include it in our program. Calculations of these processes are already available in the literature [15, 22–24], and in particular the $gg2ZZ$ and $gg2WW$ generators of refs. [22–24] can be easily interfaced to shower program, and are currently used by the experimental collaborations for this purpose.

The rest of this paper is organized as follows. In section 2, we describe the NLO calculation of the vector boson pair production processes, and the implementation of these processes in the **POWHEG BOX** framework [25]. We present our results in section 3. The effects of the **POWHEG** implementation and subsequent parton showering, common to all three vector boson pair production processes, are demonstrated for ZZ production. We also discuss the effects of anomalous trilinear boson couplings in W^+W^- and WZ production, focusing on the potential of the LHC to improve on the existing bounds on these couplings. In section 4 we give our conclusions. In the two Appendices we discuss some technical details.

2. Description of the implementation

We took the matrix elements for the Born, real and virtual amplitudes from the calculations of Ref. [12], borrowing heavily from their implementation in the **MCFM** package [14, 15]. At variance with the **MCFM** package, however, we have used the Breit-Wigner form for the off-shell vector bosons propagators

$$\frac{1}{s_V - M_V^2 + i\Gamma_V M_V}, \quad (2.1)$$

rather than the Baur-Zeppenfeld form [26]. We can also enforce the use of the running width variant (see manuals for details)

$$\frac{1}{s_V - M_V^2 + i\Gamma_V s_V/M_V}. \quad (2.2)$$

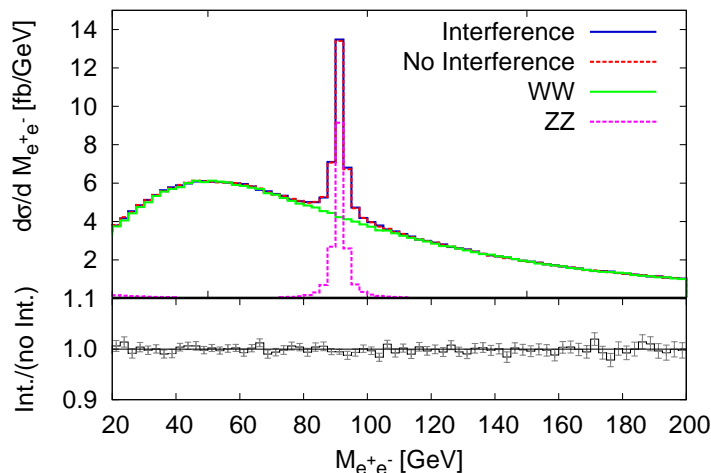


Figure 1: Distribution of $M_{e^+e^-}$ in the process $pp \rightarrow e^-e^+\nu_e\bar{\nu}_e$ at leading order and centre of mass energy of 7 TeV. This demonstrates the negligible effect of interference between W^+W^- and ZZ production of this final state. The solid green and magenta lines show the separate contribution from W^+W^- and ZZ production respectively.

We have seen, however, no appreciable differences when this last form is used.

Z/γ^* interference effects are included. Singly resonant amplitudes, which are essential if we wish to describe kinematic regions where only one of the vector bosons is resonant [15], are also included. Furthermore, we include interference terms when there are identical leptons in the final state, as in $ZZ \rightarrow e^-e^+e^-e^+$, and $ZW^\pm \rightarrow e^-e^+e^\pm\nu$. These effects are small, but become relevant when all oppositely charged lepton pairs are far off-resonance.² Interference terms of this sort never arise in W^+W^- -production. However, W^+W^- and ZZ production may lead to identical final states, such as $e^-e^+\nu_e\bar{\nu}_e$. We have studied the corresponding interference effect at leading order with Madgraph [27]. As shown for example in Fig. 1 in the case of the $M_{e^+e^-}$ distribution, such effects are completely negligible, and are therefore not included in the following. Thus, if one wishes to investigate leptonic final states like $e^-e^+\nu_e\bar{\nu}_e$, both a W^+W^- and a ZZ sample should be generated separately.

The construction of the Born phase space requires some care, in order to efficiently probe the resonance regions. In Appendix A we discuss this problem with some detail. Furthermore, as in the case of W production, a problem due to vanishing Born configurations has to be dealt with. This is explained in Appendix B.

The three programs perform quite differently. The WZ program can complete the preparation stage in roughly one hour, involving about 6 million calls, and can generate one million events (at the Les Houches level) in six hours. The WW program has similar performance, but the preparation stage may require twice as much. The ZZ program is much slower. Even without including interference for identical fermions, the preparation stage takes of the order of 6 hours, and one million events are generated in 40 hours. It

²Since interference effects are very small, and their calculation more than doubles the computing time, it is possible to switch them off by setting an appropriate flag in the `powheg.input` file. Similarly, it is possible to generate on-shell vector bosons in the zero-width approximation or to remove the single resonant diagrams, as illustrated in the implementation manuals.

is thus convenient, in this case, to use the **POWHEG BOX** facilities to run the program in parallel. Requiring interference costs more than a factor of two in execution time. The poorer performance of the ZZ program is easily tracked back to the presence of a larger number of helicity configurations that contribute to the process.

Several checks have been performed to test the correctness of the implementation. The Born and real matrix elements have been checked against **MadGraph** [27] for an arbitrary phase-space point. The ratio of the residues of the single and double poles of the virtual amplitude to the Born amplitude were compared against the analytically known expressions. The finite part of the virtual amplitude was checked against an independent Feynman diagram based program, developed by some of the authors, which uses the OPP subtraction method [28]. The **MCFM** program implements the same processes, but does not include the interference terms for identical fermions. We have thus verified that, when the interference terms are not included or not present, the NLO output of the **POWHEG** implementation, which can be obtained by setting an appropriate option in the program, is consistent within errors to that of **MCFM** for a large number of distributions. Furthermore, the **POWHEG** output at the level of the Les Houches Interface events has been compared for on shell Z bosons to the previous implementation of ref. [19]. Full agreement was found, thus demonstrating that the mechanism used by **POWHEG** to generate radiation operates in the same way as in the implementation of ref. [19], which in turn was thoroughly compared to the **MC@NLO** implementation.

3. Results

We now present some results obtained with our **POWHEG** implementation. Our basic setup for the electroweak input parameters is the following. We use M_Z , M_W and G_μ as basic parameters of the Standard Model (SM), and define all remaining quantities according to the leading order SM relations. Thus we have

$$\cos \theta_w = \frac{M_W}{M_Z}, \quad \alpha_{\text{em}} = \frac{\sqrt{2}G_\mu M_W^2}{\pi} \sin^2 \theta_w \quad (3.1)$$

This corresponds to the so called “ G_μ scheme”, advocated in ref. [29]. We adopt the following PDG [30] values for the independent parameters

$$M_Z = 91.1876 \text{ GeV}, \quad M_W = 80.399 \text{ GeV}, \quad G_\mu = 1.166364 \times 10^{-5} \text{ GeV}^{-2}. \quad (3.2)$$

For the width of the W and Z bosons, we take their LO value computed in the above scheme, except that we correct the hadronic width with a factor $(1 + \alpha_s(M_W)/\pi)$ and $(1 + \alpha_s(M_Z)/\pi)$, respectively. In this way, the branching fractions of the W/Z consistently add up to one. For the W and Z width we get 2.0997 GeV and 2.5096 GeV, respectively. These values are around half a percent away from the current PDG values [30], 2.085 ± 0.042 GeV and 2.4952 ± 0.0023 GeV, respectively, so that, in fact, the measured values could be used instead. Details can be found in the file **smcouplings.f**, which can easily be modified by users preferring other ways to implement SM couplings. As default, we set

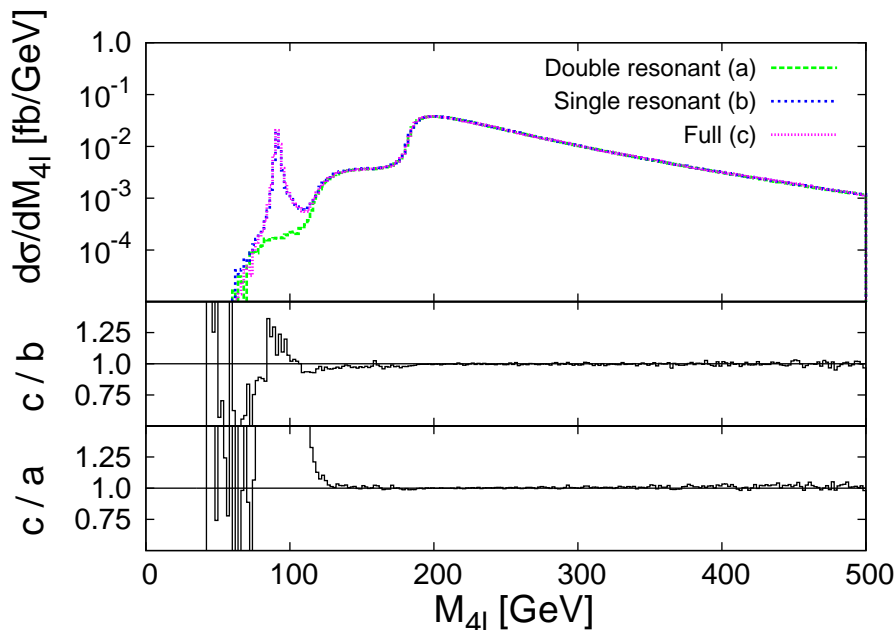


Figure 2: The effect of different levels of approximation of the calculation of $pp \rightarrow e^+e^-e^+e^-$ at 7 TeV for the invariant mass of the four-lepton system.

the factorization and renormalization scales equal to the mass of the four-lepton system, M_{4l} , and our default PDF set is the MSTW 2008 NLO [31].

The three processes we examine are very similar to one another. For each one of them we have analyzed several distributions, such as: the rapidity, pseudorapidity, transverse momentum and invariant mass of each lepton, each combination of lepton-lepton and lepton-antilepton pairs, and the four lepton system; the distance in rapidity, pseudorapidity, azimuth and ΔR distance (where $\Delta R = \sqrt{\Delta\phi^2 + \delta\eta^2}$) of all lepton-antilepton pairs; and the rapidity distribution of the hardest jet and its distance in rapidity from the four lepton system, with several transverse momentum cuts. For each distribution, the pure NLO result has been compared to the POWHEG result before the shower. All distributions behave as expected. In the present paper we illustrate a selected set of distributions with realistic cuts in the ZZ case only. We compare the various levels of approximation that one can include in the NLO calculation, and the full NLO result with the event output by POWHEG before and after the shower.

We remind the reader that the POWHEG output can be easily interfaced to all general parton shower event generators [32–35] that comply with the Les Houches event files format [36]. In the present work we use PYTHIA version 6.4.25 [32].

We illustrate our implementation of W^+W^- and WZ production by studying the effect that anomalous couplings have on these processes at the LHC.

3.1 ZZ Production

We first illustrate the differences that arise at different levels of approximation in our generator in the ZZ case. In Fig. 2 we show three predictions for the invariant mass of

	MSTW2008	CT10	NNPDF2.1
LO (fb)	14.61(1) $^{+0.19}_{-0.31}$	14.44(1) $^{+0.19}_{-0.31}$	14.61(1) $^{+0.21}_{-0.32}$
NLO (fb)	18.24(1) $^{+0.37}_{-0.31}$	17.95(1) $^{+0.35}_{-0.29}$	18.21(1) $^{+0.37}_{-0.30}$

Table 1: Total cross section for $pp \rightarrow ZZ \rightarrow e^+e^-\mu^+\mu^-$, with the only cut $M_{l+l^-} > 20$ GeV on both lepton pairs. The central values are for the scales $\mu_F = \mu_R = M_{4l}$, and the integration error in the final digit is shown in parentheses. The theoretical uncertainty is obtained by doubling and halving independently the scales μ_F and μ_R with respect to their central value, excluding the combinations that yield $\mu_F/\mu_R = 4$ and $\mu_R/\mu_F = 4$.

the four-lepton system in ZZ production, when both Z bosons decay into electrons. The cuts are as documented further on, but for the purpose of understanding the present plot, the only relevant cut is the 20 GeV one on the invariant mass of opposite sign leptons. The curve labelled as (c) is the full calculation of the four lepton production process, and thus is the more accurate result that our generator can provide. In (b), we suppress the interference effects due to identical fermion pairs in the final state. The ratio of (c) over (b) is presented in the lower panel. We see that there are sensible differences around the Z peak. This is easily understood. The singly-resonant production mechanism includes the production of a single Z boson that decays into four leptons, giving rise to the Z peak observed in the figure. In this decay process both lepton pairs are off resonance, and thus we can expect non-negligible interference effects. The knee visible in the figure at roughly $M_{4l} \approx 110$ -120 GeV is due to the onset of the production of an on-shell Z decaying into a lepton pair, with the second lepton pair arising from a Z^*/γ^* decay (this mechanism is displaced to 110-120 GeV because of the 20 GeV cut on the minimum invariant mass for a lepton pair). In this kinematic regime, with an on-shell Z decaying into a lepton pair, the interference is suppressed by the phase space. Finally, the curve labelled (a) does not include single resonant graphs or interference for identical fermions. It is in good agreement with the full result only if we are sufficiently beyond the threshold for the production of one on-shell Z boson. The approximation (b) is presently implemented in the MCFM package. The approximation (a) is implemented, for example, in PYTHIA, where off-shell effects and Z/γ^* interference are accounted for, but singly resonant graphs are not included. Because of the small differences between the single resonant (b) and the full calculation (c), for simplicity we proceed by considering decays to $e^+e^-\mu^+\mu^-$ only.

In the following, we employ a cut of $M_{l+l^-} > 20$ GeV for each electrically charged, same-flavour lepton-antilepton pair l^+l^- , which ensures that divergences due to low-virtuality photon emissions are avoided. We remark here that, if interference effects due to identical fermions are neglected, the same flavour and different flavour cross sections can be simply related; for example, the $e^+e^-\mu^+\mu^-$ cross section is twice the $e^+e^-e^+e^-$ one. We should however remember that cuts applied to the final state are generally different: in the case of $e^+e^-e^+e^-$ we limit the invariant mass of all four possible choices of oppositely charged lepton pairs, whereas in the $e^+e^-\mu^+\mu^-$ case there are only two such pairs. Thus, the cross sections are related by a factor of 2 (if we neglect interference) only if we impose additional

mass cuts on the $e^+\mu^-$ and $e^-\mu^+$ pairs in the $e^+e^-\mu^+\mu^-$ case.

In Table 1, we show the $ZZ \rightarrow e^-e^+\mu^-\mu^+$ cross-section, at leading and next-to-leading order, and show the effects of varying independently the renormalization and factorization scale by a factor of two in either direction, excluding the values that lead to a ratio of the two scales equal to 4 or 1/4. We thus consider the seven combinations: $\mu_F = \mu_R = M_{4l}$, $2\mu_F = \mu_R = M_{4l}$, $\mu_F/2 = \mu_R = M_{4l}$, $\mu_F = 2\mu_R = M_{4l}$, $\mu_F = \mu_R/2 = M_{4l}$, $2\mu_F = 2\mu_R = M_{4l}$, $\mu_F/2 = \mu_R/2 = M_{4l}$, with the first one taken as the central value. This is done for three PDF sets: MSTW08 [31], CT10 [37] and NNPDF2.1 [38]. Note that we employ NLO parton distribution functions also for LO cross-sections. The scale uncertainty is just 1-2% at leading order, and slightly smaller at next-to-leading order. We observe, however, that the NLO result does not lie within the LO scale variation band. The anomalously small scale dependence of the LO cross-section is due to the fact that the Born level process is of order zero in the strong coupling constant, and thus the only scale dependence comes from the PDFs. Furthermore, in pp collisions new quark-gluon channels open up in the NLO cross-section that compete sensibly with the LO one. Notice also that the gg -initiated contribution, which is formally of NNLO (and thus is not included in the table), is larger than the scale variation seen here. All these considerations lead to the conclusion that scale variation alone underestimates higher order effects for this process. The difference in cross-sections between different PDF sets is similar in size to the scale variation.

Experience with the POWHEG implementation of other processes has taught us that, for processes that involve only initial state radiation (ISR), one expects the effect of showers to be modest, a fact that we will verify also in the present context.

We begin by carrying out a detailed comparison of the POWHEG results at the level of the Les Houches events output (the LHE level from now on) with the NLO results. We impose the following cuts: the highest p_t lepton must have $p_t > 20$ GeV, and the other three hardest leptons must have $p_t > 10$ GeV. We also require for the lepton rapidities that $|\eta| < 2.5$. Jets are reconstructed using the anti- k_t algorithm [39] as implemented in FastJet [40], with $R = 0.6$. In Fig. 3, we show results obtained by analyzing the LHE files directly, without further showering, compared to the NLO result. Six distributions are presented: M_{Z_1} , M_{Z_2} , M_{4l} , p_{t,Z_1} , y_{e^-} , and y_{Z_1} , where y is rapidity and M denotes an invariant mass distribution. For every phase space point, we assign Z_1 to the lepton pair of the same flavour whose invariant mass is closest to M_Z and label the other lepton pair as Z_2 . This explains the difference between the first two plots. In fact, the lepton pair closest to the Z mass tends to have a much reduced contribution from γ^* production. In general, we see good agreement, at the level of few percent, between the two predictions for these inclusive quantities. Other inclusive variables exhibit a similar behaviour.

We now show the transverse momentum distribution of the four lepton system, $p_{t,4l} = |\sum_l \vec{p}_{t,l}|$, in the left plot of Fig. 4, which at NLO is identical to the transverse momentum distribution of the jet. We see large differences between NLO and LHE results. At low $p_{t,4l}$, the LHE result is much smaller than the NLO one. This fact is typically understood as originating from the Sudakov suppression which is present in the POWHEG output, but not in the NLO result, which diverges at small $p_{t,4l}$. At large $p_{t,4l}$ the LHE result overshoots the NLO one by about 50%. An enhancement of the large $p_{t,4l}$ tail of the POWHEG distribution

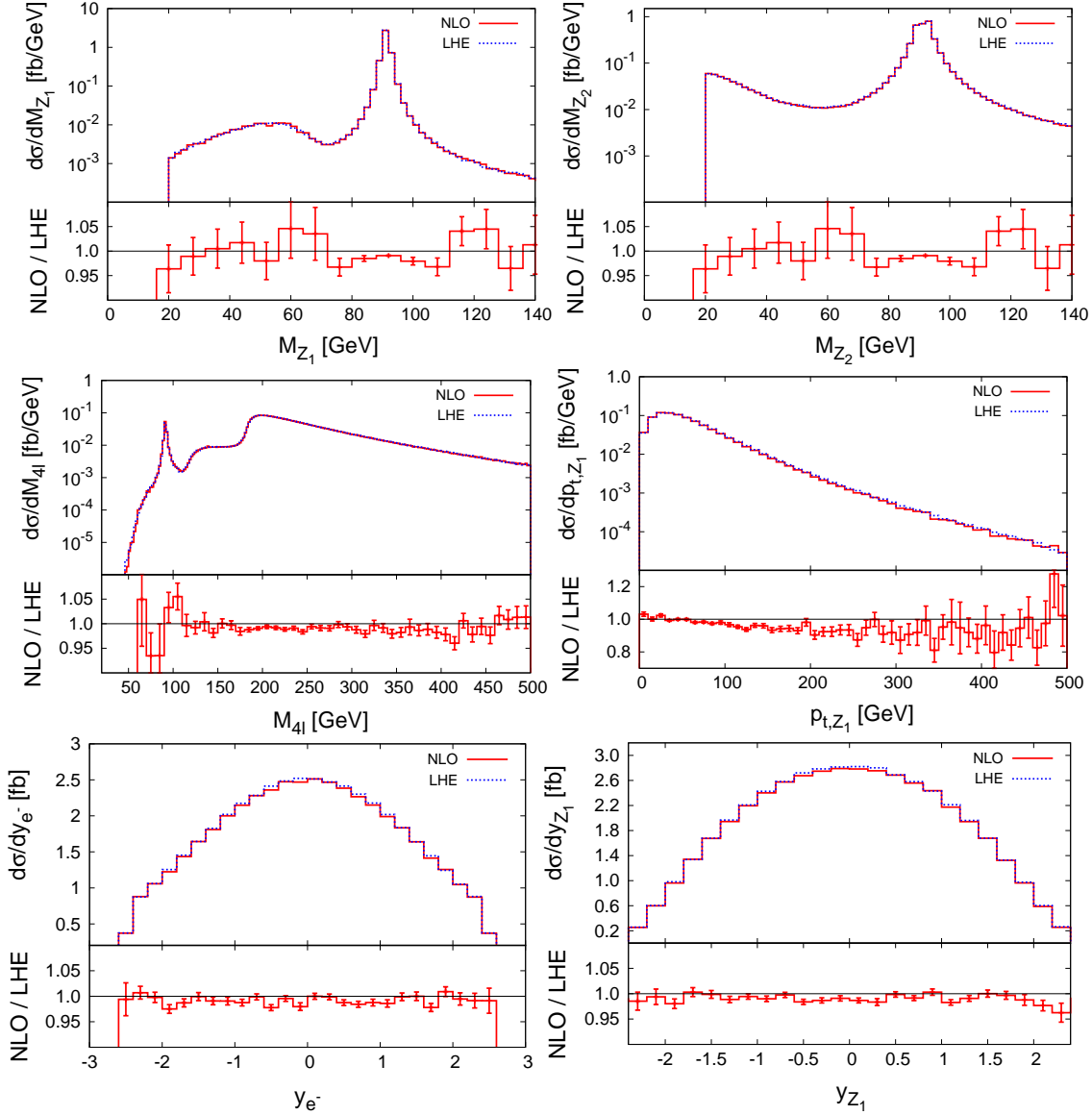


Figure 3: Comparison of NLO to LHE events for $pp \rightarrow e^+e^-\mu^+\mu^-$ at 7 TeV for a number of observables, for our default set of cuts. The definitions of Z_1 and Z_2 are given in the text.

is also observed in processes like single vector boson production and gluon-fusion Higgs production. The origin of this effect is discussed in [41,42]. In essence, in POWHEG, the large transverse momentum distribution in the real emission process is enhanced by the NLO K-factor. We thus expect an enhancement of the order of ~ 1.25 in our case. However, we see that this effect accounts only for a fraction of the enhancement observed in the plot. The remaining enhancement is easily traced to arise from the different choice of scales used in the NLO calculation and in the generation of LHE events, the former being equal to the invariant mass of the four lepton system, and the latter being instead taken equal to its transverse momentum. These points are illustrated in the right plot of Fig.

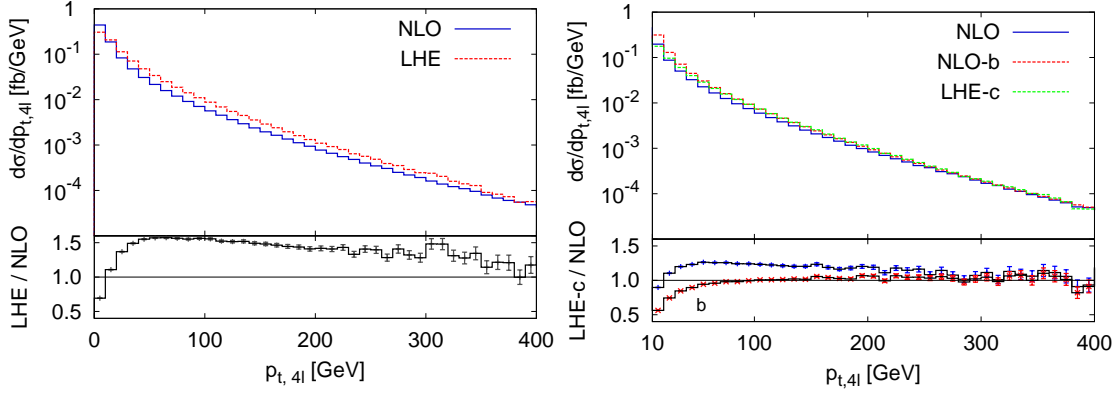


Figure 4: In the left plot, we compare the transverse momentum distribution of the four-lepton system in the process $pp \rightarrow e^+e^-\mu^+\mu^-$ at 7 TeV, obtained with the fixed order NLO result, and at the Les Houches events level. On the right plot the same comparison is carried out for the fixed order NLO result (NLO), and the fixed order NLO calculation with the renormalization and factorization scale in the real contribution set to $p_{t,4l}$ (NLO-b), versus a **POWHEG** result at the Les Houches event level with the **bornonly** option set (LHE-c). In the lower panel, the curve labelled b is the ratio of LHE-c/NLO-b.

4 where we plot the same quantity using the **bornonly** option in **POWHEG**³ compared to the standard NLO result, and to the NLO result obtained by setting the factorization and renormalization scales equal to $p_{t,4l}$ in the real contribution. The ratio of the **POWHEG** result with the **bornonly** option set, over the NLO result with the $p_{t,4l}$ scale choice, eliminates two causes of the difference (i.e. the different scale choice, and the \bar{B}/B factor), leaving only the Sudakov effect, represented in the figure by the ratio of the LHE-c versus the NLO-b result (curve marked as b in the lower panel). Observe that the ratio LHE-c/NLO is about 25% lower than the LHE/NLO ratio, thus showing that the K-factor effect is indeed of the order of 25%. Finally, we remark that the scale choice $\mu = p_{t,4l}$ is more appropriate for the description of the radiation transverse momentum than our default one in the NLO calculation. Thus, in this respect **POWHEG** does the right thing.

We now examine, for the same observables shown in Fig. 3, the effect of a subsequent shower, obtained by interfacing the **POWHEG** output with **PYTHIA**. When showering, we turn off electromagnetic radiation.⁴ The results can be seen in Fig. 5. As expected, we see very little effect from the parton shower for these observables. We remark that in **POWHEG**, by construction, the invariant mass of the two- and four-lepton systems are in fact the same at the NLO-level, LHE-level, and after parton shower (regardless of the shower program).

Turning now to exclusive variables, we show in Fig. 6 the distribution of the jet pseudo-rapidity η_j , and the rapidity difference between the jet and the ZZ system, y_{jZZ} , comparing LHE with both NLO and the effects of showering with **PYTHIA**. In addition to the lepton cuts already described we have jet cuts of $p_{t,j} > 20$ GeV, and $|\eta_j| < 3.5$. We see a noticeable

³This option eliminates the K-factor enhancement by replacing $\bar{B} \rightarrow B$ in the **POWHEG** code, see [41, 42] for details.

⁴This is adequate in this work for purpose of illustration, since an experiment will generally correct the lepton energy for electromagnetic radiation emitted collinearly.

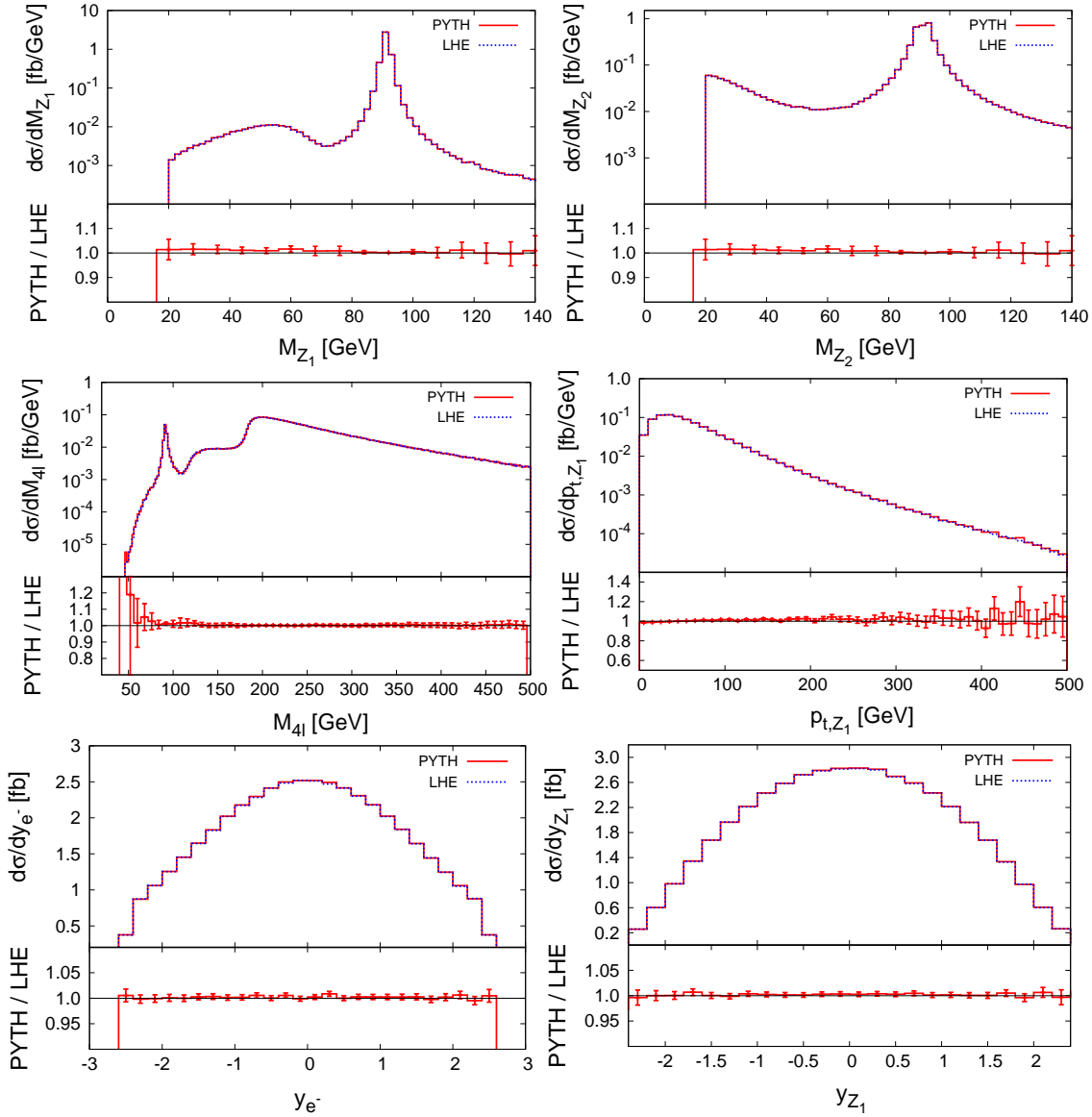


Figure 5: Comparison of LHE to PYTHIA showered events for $pp \rightarrow e^+e^-\mu^+\mu^-$ at 7 TeV for a number of observables, for our default set of cuts. The definitions of Z_1 and Z_2 are given in the text.

difference between NLO and LHE results in this distribution. This is a consequence of the jet p_t -cut and of the difference in the jet p_t distribution at NLO and LHE level (see Fig. 4). However, a subsequent parton shower has a small effect on the LHE results.

3.2 W^+W^-/WZ Production

In this Section we present predictions for W^+W^-/WZ production decaying to four leptons. As for ZZ production, the NLO calculation includes Z/γ^* interference, single resonant diagrams, and when relevant, interference due to identical leptons.

In Tables 2 and 3, we show the cross-sections for $WZ \rightarrow e^+e^-\mu^-\bar{\nu}_\mu$ and $W^+W^- \rightarrow$

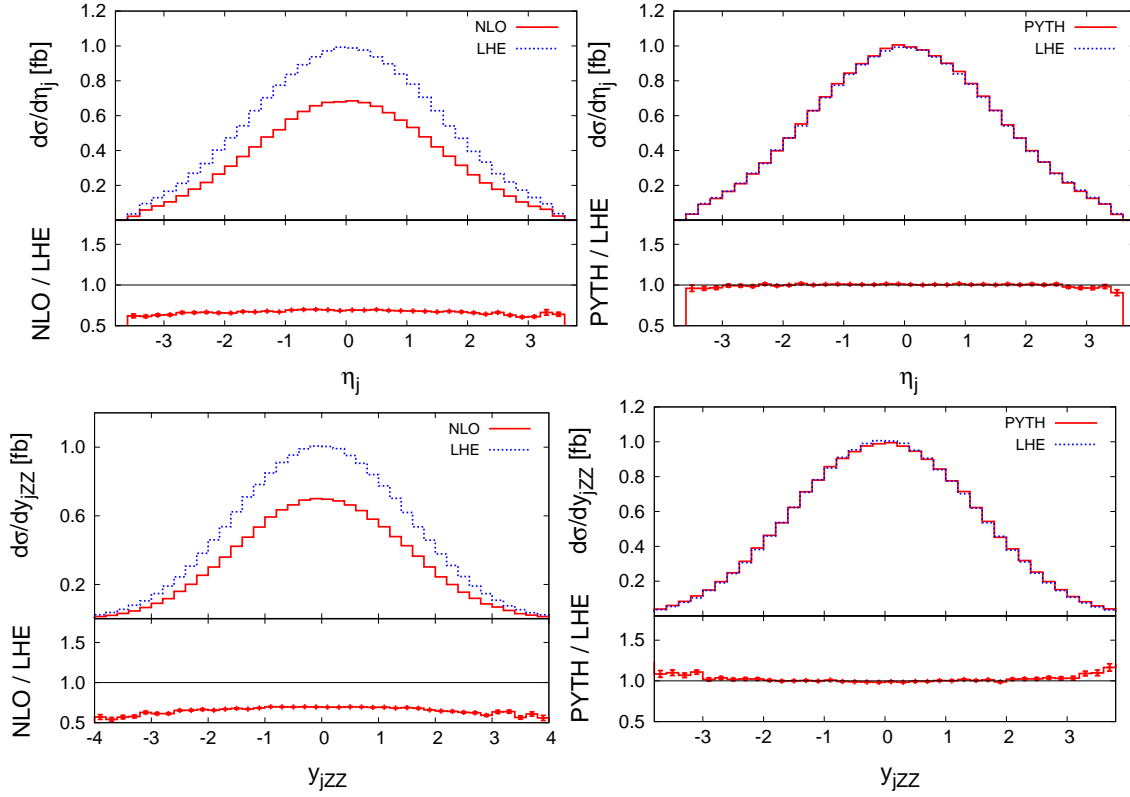


Figure 6: The pseudorapidity of the jet η_j (top row) and the rapidity difference between the jet and the ZZ system, y_{jzz} (bottom row), for $pp \rightarrow e^+e^-\mu^+\mu^-$ at 7 TeV. Additional cuts of $p_{t,j} > 20$ GeV and $|\eta_j| < 3.5$ are applied. The first column shows a comparison between NLO and LHE, and the second column a comparison between the pure LHE and the events showered with PYTHIA.

	MSTW2008	CT10	NNPDF2.1
LO (fb)	$18.53(3)^{+0.09}_{-0.25}$	$17.95(3)^{+0.05}_{-0.24}$	$18.30(3)^{+0.15}_{-0.24}$
NLO (fb)	$27.03(4)^{+0.94}_{-0.78}$	$26.00(3)^{+0.91}_{-0.65}$	$26.73(4)^{+0.88}_{-0.73}$

Table 2: As in table 1 for $pp \rightarrow W^-Z \rightarrow \mu^-\bar{\nu}_\mu e^+e^-$, with the only cut $M_{e^+e^-} > 20$ GeV on the lepton pair originating from the Z boson.

	MSTW2008	CT10	NNPDF2.1
LO (fb)	$373.8(1)^{+1.2}_{-3.4}$	$368.7(1)^{+1.3}_{-3.4}$	$375.2(1)^{+1.6}_{-3.8}$
NLO (fb)	$498.7(2)^{+13}_{-10}$	$490.0(2)^{+12}_{-10}$	$499.8(2)^{+12}_{-10}$

Table 3: As in table 1 for $pp \rightarrow W^+W^- \rightarrow e^+\nu_e\mu^-\bar{\nu}_\mu$, with no cuts applied.

$\mu^-\nu_\mu e^+\bar{\nu}_e$, for MSTW2008, CT10 and NN2.1 NLO PDF sets. The theoretical error due to scale variation is computed with the same method of table 1. For WZ and W^+W^- production, we find scale uncertainties of around 1% at leading order, and 2-3% at next-

to-leading order. Again the NLO result is not contained in the LO scale variation band. This pattern was already observed and discussed in the ZZ production case.

Our implementation also allows one to study effects due to non Standard-Model like (anomalous) WWZ and $WW\gamma$ couplings. While the LHC will probe new physics at the TeV scale directly, anomalous trilinear gauge couplings (ATGCs) indirectly probe physics at larger scales, since they arise when high-energy degrees of freedom are integrated out. Both the Tevatron [7,8,43] and LEP [44] were able to place quite stringent bounds on anomalous trilinear couplings. However, since their effects are enhanced at high energies, one may expect even better bounds from the LHC. Indeed, CMS already presented bounds on the anomalous couplings appearing in an effective Lagrangian with the parametrization of ref. [45] (HISZ from now on) without form factors [11]. It is then interesting to understand when the LHC running at 7 TeV will be in a position to improve on existing Tevatron and LEP bounds [46].

Following ref. [45,47,48], we parametrize the most general terms for the WWV vertex ($V = \gamma, Z$) in a Lagrangian that conserves C and P as

$$\mathcal{L}_{\text{eff}} = ig_{WWV} \left(g_1^V (W_{\mu\nu}^* W^{\mu\nu} V^\nu - W_{\mu\nu} W^{*\mu\nu} V^\nu) + \kappa^V W_\mu^* W_\nu V^{\mu\nu} + \frac{\lambda^V}{M_W^2} W_{\mu\nu}^* W_\rho^\nu V^{\rho\mu} \right), \quad (3.3)$$

where $W_{\mu\nu} = \partial_\mu W_\nu - \partial_\nu W_\mu$, $g_{WWZ} = -e \cot\theta_W$ and $g_{WW\gamma} = -e$. In the SM $g_1^V = \kappa_1^V = 1$, and $\lambda^V = 0$. Any departure from these values would be a sign of new physics. Therefore anomalous couplings are usually written in terms of the deviation from their SM value, e.g. $\Delta g_1^V = g_1^V - 1$ etc. In our POWHEG generator, all six parameters can be set independently. If one imposes gauge invariance under abelian (electromagnetic) gauge transformations, the parameter Δg_1^γ vanishes. This still leaves five independent anomalous couplings. The LEP groups use a parametrization in which the number of independent couplings reduces to three. This is a consequence of only including operators of up to dimension six in their effective Lagrangian. One can write the couplings in terms of the three parameters α_W , $\alpha_{W\phi}$ and $\alpha_{B\phi}$

$$\Delta g_1^Z = \frac{\alpha_{W\phi}}{\cos^2\theta_W}, \quad \lambda^\gamma = \lambda^Z = \alpha_W, \quad \Delta\kappa^\gamma = \alpha_{W\phi} + \alpha_{B\phi}, \quad \Delta\kappa^Z = \alpha_{W\phi} - \tan^2\theta_W \alpha_{B\phi}. \quad (3.4)$$

Note that this implies the relation

$$\Delta\kappa^Z = \Delta g_1^Z - \Delta\kappa^\gamma \tan^2\theta_W. \quad (3.5)$$

In the HISZ model [45], it was also suggested that one may set $\alpha_{W\phi} = \alpha_{B\phi}$ as a further simplification, leaving only two independent parameters. This modified setup is sometimes used in experimental searches.

In the presence of anomalous couplings, the effective Lagrangian of eq. (3.3) gives rise to interactions that violate unitarity at high energy. Thus, in order to achieve a more realistic parametrization, the couplings are multiplied by form factors, that embody the effects arising from integrating out the new physics degrees of freedom. The precise details of the form factors therefore depend on the particular model considered. Paralleling here

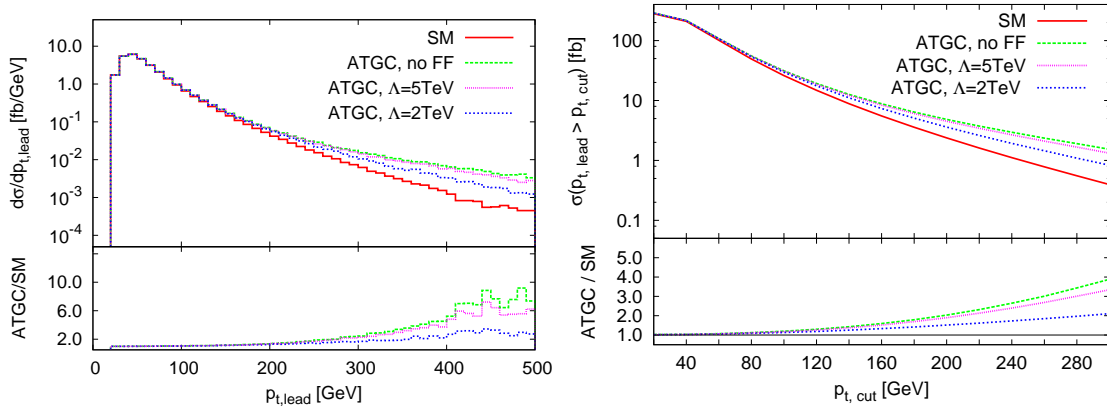


Figure 7: The p_t distribution for the leading lepton in W^+W^- -production is shown on the left, and the integrated cross-section as a function of the cut on the transverse momentum of the leading lepton is shown on the right. The results are shown using Standard Model couplings (in red, labeled ‘SM’), as well as with the anomalous couplings of eq. (3.7) (in green, labeled ‘ATGC, no FF’). The effect of a form factor given in eq. (3.6) is also shown, both for a value of $\Lambda = 5$ TeV and $\Lambda = 2$ TeV (in pink and blue respectively).

the discussion of ref. [49], we assume that all anomalous coupling Δg are modified as

$$\Delta g \rightarrow \frac{\Delta g}{(1 + M_{VV}^2/\Lambda^2)^2}, \quad (3.6)$$

where M_{VV} is the invariant mass of the vector boson pair and Λ is the scale of the new physics.

In the LEP study of ref. [50] the value of one or two of the parameter(s) is fixed to their SM values, and determines the range of values of the remaining parameter(s) consistent with their data. We choose the maximum deviation of *all* parameters from their SM values allowed by these fits. While it is true that this point in parameter space would lie outside the LEP bounds where all three parameters are allowed to vary, we choose it for illustrative purposes.

The values of the parameters are

$$\Delta g^Z = -0.027, \quad \Delta \lambda^Z = \Delta \lambda^\gamma = -0.044, \quad \Delta \kappa^\gamma = -0.112, \quad (3.7)$$

and where (using the LEP groups parametrization) $\Delta \kappa^Z$ is obtained from the above using eq. (3.5). We note that these values for the ATGCs also fall within the unitarity bounds of ref. [51] for $\Lambda \lesssim 7$ TeV. In the left-hand plot of Fig. 7 we show the p_t distribution for the hardest lepton (which is known to be very sensitive to ATGCS) in W^+W^- -production using the above ATGCs, with different values of the form factor parameter ($\Lambda = 2$ TeV, 5 TeV and ∞). The effect of the anomalous couplings is evident in the high- p_t tail of the distribution. The form factor damps the effect of the ATGCs. Its impact increases with decreasing Λ , while $\Lambda = \infty$ corresponds to no form factor. In the right-hand plot of Fig. 7, we show the integrated cross-section as a function of the cut on the p_t of the leading lepton. Fig. 7 gives an indication of the kind of signal one would see at the LHC. Depending upon

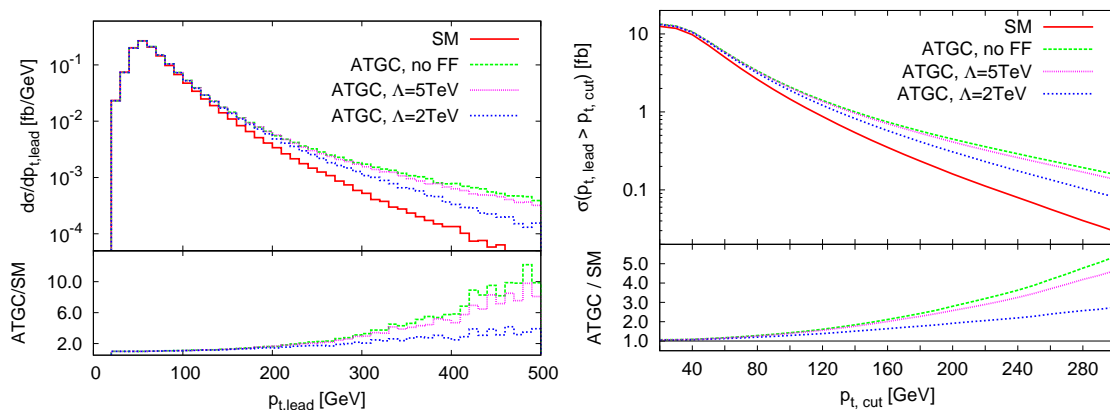


Figure 8: As in Fig. 7 for W^-Z production.

the precise form of the new physics, the signal would lie somewhere between the $\Lambda = 2$ TeV and $\Lambda = \infty$ predictions. We note that in the region $p_t > p_{t,\min}$, with $150 \lesssim p_{t,\min} \lesssim 250$ GeV, the cross section is strongly affected by the anomalous couplings. Furthermore, its value is of the order of 1 to 10 fb, and thus such a difference should be observable with a few inverse femtobarns of data. It may then be possible for the LHC to improve on the LEP bounds on anomalous trilinear boson couplings already by the end of the year.

Similar results are obtained in the case of WZ production, and are shown in Fig. 8 for W^-Z . This process is sensitive only to the WWZ tri-linear coupling and not to the $WW\gamma$ couplings. In this case the cross section is smaller and one expects to make less stringent bounds than in the W^+W^- study.

4. Conclusion

We have implemented the production of vector boson pairs W^+W^- , $W^\pm Z$ and ZZ in the POWHEG BOX. Off-shell effects, Z/γ^* interference, single resonant amplitudes and interference between same-flavour leptons have all been included. The only effect not included is the interference between W^+W^- and ZZ processes, when both decay to same-flavour leptons and neutrinos. We have, however, shown that this interference is entirely negligible, so that it suffices to consider these processes separately. We have shown that, for variables inclusive in the hardest jet (or equivalently in the radiated parton), there is very little difference between NLO and LHE results, whereas noticeable differences arise for variables that probe the hardest jet. Neither kind of observable is much affected by the subsequent parton shower.

Our POWHEG implementation allows the study of the effect of anomalous trilinear boson couplings in WZ and W^+W^- production. We demonstrated this for both processes at the LHC with $\sqrt{s} = 7$ TeV, and looked at the distribution of the p_t of the hardest lepton. We saw that a set of anomalous couplings allowed by the LEP bounds leads to a large deviation from the Standard Model result in the high p_t bins of this distribution, to such an extent that the LHC may be able to probe this by the end of the present year.

We have not included in this work the $W\gamma$ or $Z\gamma$ processes with an on-shell photon. This is because NLO calculations with final state on shell photons have to dealt with in a different way. Photons can be radiated in the collinear direction by light quarks, and thus generate singularities that require special attention. Including photons in a POWHEG generator is however possible, and in ref. [52], for example, the $\gamma\gamma$ production process was implemented. We thus defer this problem to future work.

Finally, the code for our generators has been made available at the POWHEG BOX website <http://powhegbox.mib.infn.it>.

Acknowledgments We wish to thank J. Campbell, S. Dittmaier, K. Ellis, F. Maltoni, R. Frederix and G. Passarino for useful exchanges. This work is supported by the British Science and Technology Facilities Council, by the LHCPhenoNet network under the Grant Agreement PITN-GA-2010-264564 and by the European Research and Training Network (RTN) grant Unification in the LHC ERA under the Agreement PITN-GA-2009-237920.

A. Phase space sampling

Although the POWHEG implementation of the processes we consider is relatively straightforward, some care is needed in the generation of the Born phase space, to ensure that the resonant regions are probed efficiently. Thus, when implementing processes with no lepton interference, like $ZZ \rightarrow e^+e^-\mu^+\mu^-$, the phase space generator should include the virtuality of the e^+e^- and $\mu^+\mu^-$ pairs as integration variables, so that the importance sampling can be performed near the Z peak or for low invariant mass, where the pole of the photon propagator starts to count. In ZZ and WZ production, a cut on the lepton pair mass for oppositely charged same flavour leptons must be imposed, in order to stay away from the photon pole.

When lepton interference is present, like in $ZZ \rightarrow e^+e^-e^+e^-$, there are two ways to assign the leptons to the vector resonance, and using all the corresponding mass combinations as integration variables becomes too cumbersome. In this case, in order to maintain an efficient importance sampling, we do the following. Calling 1 and 2 the two possible resonance assignments, we multiply the cross section by a factor $2F_2/(F_1 + F_2)$, where the $F_{1/2}$ are factors that suppress the vector poles for the 1 or 2 resonance assignment. This is possible since the two resonance assignments differ only by a permutation of identical fermions, and the cross section is symmetric under $1 \leftrightarrow 2$ exchange. After multiplying the cross section by this factor, the poles of the second region are suppressed, and one can adopt a phase space importance sampling as if there was only the resonance assignment 1. In case of the $ZZ \rightarrow e^+(1)e^-(2)e^+(3)e^-(4)$ process, for example, the function F_1 , relative to the resonance assignment (1, 2), (3, 4) is chosen equal to

$$F_1 = \{s_{12} [(s_{12} - M_Z^2)^2 + \Gamma_Z^2 M_Z^2] \times s_{34} [(s_{34} - M_Z^2)^2 + \Gamma_Z^2 M_Z^2]\}^2, \quad (\text{A.1})$$

while F_2 is obtained by replacing $1 \leftrightarrow 3$. In case of the $ZW \rightarrow e^+(1)e^-(2)e^+(3)\nu_e(4)$

process, we have

$$F_1 = \left\{ s_{12} \left[(s_{12} - M_Z^2)^2 + \Gamma_Z^2 M_Z^2 \right] \times \left[(s_{34} - M_W^2)^2 + \Gamma_W^2 M_W^2 \right] \right\}^2, \quad (\text{A.2})$$

for the region $(1, 2), (3, 4)$. For F_2 one replaces again $1 \leftrightarrow 3$. In order to avoid possible errors in the analysis, the output at the level of Les Houches Interface is symmetrized again by randomly permuting the kinematics of the identical final state leptons.

B. Born zeros

All three production processes considered here have a Born cross section that vanishes in particular kinematic regions due to angular momentum conservation. In fact, since the vector interaction preserves chirality, the incoming quark-antiquark system has total spin equal to 1 in magnitude. If we consider the final state configuration where all leptons are parallel to the incoming quark, the whole system is symmetric under azimuthal rotations, and thus the angular momentum component along the collision axis equals the sum of the spins, and should be preserved. On the other hand, the final state leptons can be divided into two pairs with opposite helicity, thus yielding two systems with total spin 1 (in absolute value) along the collision axis. Since the sum of the two spin 1 system yields either 2 or zero, angular momentum is violated in this configuration, and the amplitude must vanish. This property can be easily verified numerically.

It was first pointed out in ref. [53] that problems can arise in the POWHEG formalism if the Born cross section vanishes or becomes particularly small in certain kinematic regions. We briefly recall the nature of this problem in the following.

The basic POWHEG cross section formula can be written as

$$d\sigma = \bar{B}(\Phi_B) d\Phi_B \left[\Delta_{t_0}^s(\Phi_B) + \Delta_t^s(\Phi_B) \frac{R^s(\Phi)}{B(\Phi_B)} d\Phi_r \right] + [R(\Phi) - R^s(\Phi)] d\Phi, \quad (\text{B.1})$$

where the real phase space is factorized in terms of the underlying Born Φ_B and the radiation Φ_r phase space: $d\Phi = d\Phi_r d\Phi_B$, and B , R and V are the Born, real and virtual amplitudes. R^s is an approximation to the real amplitude such that $0 \leq R^s \leq R$, and that $R^s \rightarrow R$ in the limit of soft or collinear singularities. The choice $R^s = R$ is also allowed, and is often used. The variable t represents, in the present case, the transverse momentum of the radiated parton relative to the collision axis (thus t is a function of the phase space point), and t_0 is a non-perturbative cutoff (of the order of a typical hadronic scale) on this variable. Furthermore

$$\bar{B}(\Phi_B) = B(\Phi_B) + \left[V(\Phi_B) + \int R^s(\Phi) d\Phi_r \right], \quad (\text{B.2})$$

and

$$\Delta_{t_l}^s(\Phi_B) = \exp \left[- \int_{t > t_l} \frac{R^s(\Phi)}{B(\Phi_B)} d\Phi_r \right]. \quad (\text{B.3})$$

The Born term may become particularly small in certain kinematic regions; for example, if it vanishes for symmetry reasons. Besides the present case, another example of a behaviour

of this kind is the case of W production and decay, where there is a zero in the Born cross section if the outgoing lepton is anti-parallel to the incoming quark [53], which is due to angular momentum conservation and to the left-handed nature of charged currents. It may then turn out that the \bar{B} function does not vanish in the same region, due to the presence of the real term in eq. (B.2). From eq. (B.1), we see that, in this case, away from the Sudakov region, the real contribution may be enhanced by a factor \bar{B}/B . The **POWHEG BOX** has a built-in mechanism to deal with this problem. If the flag **withdamp** is set, R^s is chosen to vanish in the regions where R differs too much (by more than a factor of 5) from its collinear or soft approximation, which are proportional to the underlying Born cross section. The contribution $R - R^s$, being non-singular, is then added independently. We thus conclude that the **withdamp** flag should also be activated in the processes we are considering.

In practice, it turns out that the effect of the **withdamp** flag is much more important in the W^+W^- and in the WZ case, than in the ZZ case. This fact can be easily understood in the WZ case, where another region of vanishing Born cross section can be found which is less suppressed by phase space. Assume we have an incoming d quark in the positive rapidity direction, colliding with a \bar{u} . In WZ production only the left handed component of the incoming d , and the right handed component of the incoming \bar{u} , contribute, so that the incoming particles have a definite angular momentum projection along the collision axis equal to 1. Consider now the kinematic region where the W^- decay products are aligned along the collision axis, with the negative lepton in the negative rapidity direction. Again, the negative lepton is left handed, while the antineutrino is right handed. Thus the system has angular momentum projection along the collision axis equal to -1. Since the Z must also have zero transverse momentum, in order to balance the angular momentum component along the collision axis it should have spin 2, which is impossible. Thus this region is also suppressed, irrespective of the direction of the decay products of the Z .

The W^+W^- case is not as simple, since here there are two amplitudes that contribute: one with the two W s emerging from the incoming fermion line (t-channel amplitude), and the other with the two W s arising from the WWZ or $WW\gamma$ vertex, the Z/γ^* being attached to the incoming quark line (s-channel amplitude). The same argument applied to the WZ case also applies to the t -channel amplitude. We can use a similar argument to show that the s -channel amplitude vanishes when the decay products of the two W 's travel along the same line, with the neutrino of one W is aligned to the lepton of the other. In this case, the decay system has angular momentum projection in the line of decay equal to 2, and it can't therefore arise from a virtual Z or γ decay. Although we cannot conclude that the full amplitude vanishes in either direction, even here we expect a strong kinematic suppression of the Born amplitude in certain regions.

In Fig. 9, we show the transverse momentum distribution of the four lepton system in ZZ and W^+W^- production if the **withdamp** flag is not set ⁵ (the effect in WZ production is

⁵Because of the radiation zeroes, the upper bound of radiation tends to diverge as we increase the number of points used to compute it (i.e. the **nubound** variable in the **powheg.input** file). On the other hand, with a limited number of points we still get a relatively small rate of upper bound violations in the generation of radiation, so that these distributions can be nevertheless computed.

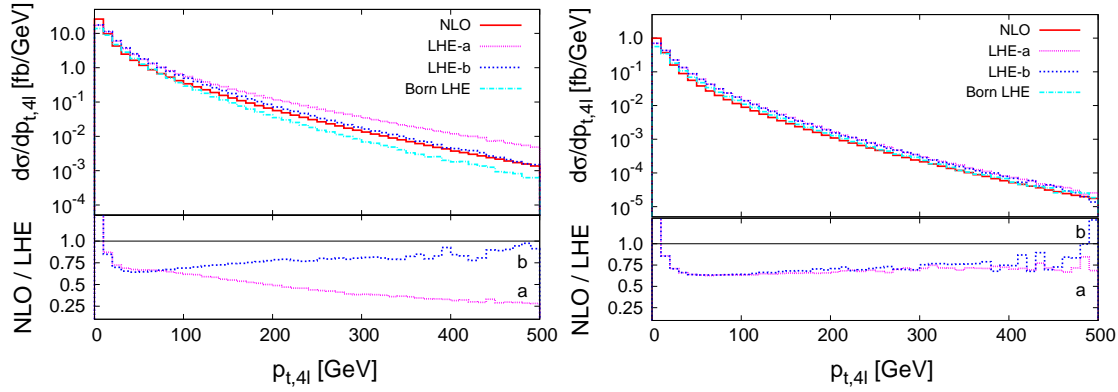


Figure 9: Distribution of $p_{t,4l}$ for $pp \rightarrow W^+W^- \rightarrow e^+\nu_e\mu^-\bar{\nu}_\mu$ and $pp \rightarrow ZZ \rightarrow e^+e^-\mu^+\mu^-$, at centre of mass energy 7 TeV. The NLO results are shown in red, and LHE results using only the Born cross-section to generate events are shown in light blue. Also shown are the NLO LHE results with damping (in dark blue and labeled ‘LHE-b’) and without damping (in magenta and labeled ‘LHE-a’). The bottom plot shows the ratio of the NLO results to the LHE results with damping (dark blue, labeled ‘b’), and the ratio of the NLO results to the LHE results without damping (magenta, labeled ‘a’).

very similar to that in W^+W^- production and is not shown). While we find a very modest effect in the ZZ case, in the W^+W^- case we find large enhancement of the differential cross section as a function of the LHE transverse momentum of the hardest parton. We also find that this anomalous behaviour disappears if we set $\bar{B} = B$ in POWHEG (this is achieved by setting the flag `bornonly` to 1 in the `powheg.input` file). Thus, the anomalous growth is due to a large \bar{B}/B ratio in some kinematical regions.

References

- [1] V. M. Abazov *et al.* [D0 Collaboration], Phys. Rev. Lett. **94** (2005) 151801 [Erratum-ibid. **100** (2008) 139901] [arXiv:hep-ex/0410066].
- [2] V. M. Abazov *et al.* [D0 Collaboration], Phys. Rev. Lett. **95** (2005) 141802 [arXiv:hep-ex/0504019].
- [3] D. E. Acosta *et al.* [CDF Collaboration], Phys. Rev. Lett. **94**, 211801 (2005) [arXiv:hep-ex/0501050].
- [4] V. M. Abazov *et al.* [D0 Collaboration], Phys. Rev. D **76** (2007) 111104 [arXiv:0709.2917 [hep-ex]].
- [5] A. Abulencia *et al.* [CDF Collaboration], Phys. Rev. Lett. **98**, 161801 (2007) [arXiv:hep-ex/0702027].
- [6] T. Aaltonen *et al.* [CDF Collaboration], Phys. Rev. Lett. **100**, 201801 (2008) [arXiv:0801.4806 [hep-ex]].
- [7] T. Aaltonen *et al.* [CDF Collaboration], Phys. Rev. Lett. **104**, 201801 (2010) [arXiv:0912.4500 [hep-ex]].
- [8] V. M. Abazov *et al.* [D0 Collaboration], Phys. Rev. Lett. **103** (2009) 191801 [arXiv:0904.0673 [hep-ex]].

- [9] V. M. Abazov *et al.* [D0 Collaboration], arXiv:1104.3078 [hep-ex].
- [10] G. Aad *et al.* [ATLAS Collaboration], arXiv:1104.5225 [hep-ex].
- [11] S. Chatrchyan *et al.* [CMS Collaboration], Phys. Lett. B **699** (2011) 25 [arXiv:1102.5429 [hep-ex]].
- [12] L. J. Dixon, Z. Kunszt and A. Signer, Nucl. Phys. B **531** (1998) 3 [arXiv:hep-ph/9803250].
- [13] U. Baur, T. Han, J. Ohnemus, Phys. Rev. **D53** (1996) 1098-1123. [hep-ph/9507336].
- [14] J. M. Campbell and R. K. Ellis, Phys. Rev. D **60** (1999) 113006 [arXiv:hep-ph/9905386].
- [15] J. M. Campbell, R. K. Ellis and C. Williams, JHEP **1107** (2011) 018 [arXiv:1105.0020 [hep-ph]].
- [16] S. Frixione and B. R. Webber, JHEP **0206** (2002) 029 [arXiv:hep-ph/0204244].
- [17] P. Nason, JHEP **0411** (2004) 040 [arXiv:hep-ph/0409146].
- [18] S. Frixione, P. Nason and C. Oleari, JHEP **0711** (2007) 070 [arXiv:0709.2092 [hep-ph]].
- [19] P. Nason and G. Ridolfi, JHEP **0608** (2006) 077 [arXiv:hep-ph/0606275].
- [20] K. Hamilton, JHEP **1101** (2011) 009 [arXiv:1009.5391 [hep-ph]].
- [21] S. Hoche, F. Krauss, M. Schonherr and F. Siegert, JHEP **1104** (2011) 024 [arXiv:1008.5399 [hep-ph]].
- [22] T. Binoth, N. Kauer, P. Mertsch, Proceedings of the SPIRES Conference C08/04/07.1, [arXiv:0807.0024 [hep-ph]].
- [23] T. Binoth, M. Ciccolini, N. Kauer, M. Kramer, JHEP **0503** (2005) 065. [hep-ph/0503094].
- [24] T. Binoth, M. Ciccolini, N. Kauer and M. Kramer, JHEP **0612** (2006) 046 [arXiv:hep-ph/0611170].
- [25] S. Alioli, P. Nason, C. Oleari and E. Re, JHEP **1006** (2010) 043 [arXiv:1002.2581 [hep-ph]].
- [26] U. Baur and D. Zeppenfeld, Phys. Rev. Lett. **75** (1995) 1002 [arXiv:hep-ph/9503344].
- [27] J. Alwall *et al.*, JHEP **0709** (2007) 028 [arXiv:0706.2334 [hep-ph]].
- [28] G. Ossola, C. G. Papadopoulos and R. Pittau, JHEP **0805**, 004 (2008) [arXiv:0802.1876 [hep-ph]].
- [29] S. Dittmaier and M. I. Kramer, Phys. Rev. D **65** (2002) 073007 [arXiv:hep-ph/0109062].
- [30] K. Nakamura *et al.* [Particle Data Group], J. Phys. G **37** (2010) 075021.
- [31] A. D. Martin, W. J. Stirling, R. S. Thorne and G. Watt, Eur. Phys. J. C **63** (2009) 189 [arXiv:0901.0002 [hep-ph]].
- [32] T. Sjostrand, S. Mrenna and P. Z. Skands, JHEP **0605** (2006) 026 [arXiv:hep-ph/0603175].
- [33] G. Corcella *et al.*, JHEP **0101** (2001) 010 [arXiv:hep-ph/0011363].
- [34] M. Bahr *et al.*, Eur. Phys. J. C **58** (2008) 639 [arXiv:0803.0883 [hep-ph]].
- [35] T. Sjostrand, S. Mrenna and P. Z. Skands, Comput. Phys. Commun. **178** (2008) 852 [arXiv:0710.3820 [hep-ph]].
- [36] J. Alwall *et al.*, Comput. Phys. Commun. **176** (2007) 300 [arXiv:hep-ph/0609017].

- [37] H. L. Lai, M. Guzzi, J. Huston, Z. Li, P. M. Nadolsky, J. Pumplin and C. P. Yuan, *Phys. Rev. D* **82** (2010) 074024 [arXiv:1007.2241 [hep-ph]].
- [38] R. D. Ball *et al.*, *Nucl. Phys. B* **849** (2011) 296 [arXiv:1101.1300 [hep-ph]].
- [39] M. Cacciari, G. P. Salam and G. Soyez, *JHEP* **0804** (2008) 063 [arXiv:0802.1189 [hep-ph]].
- [40] M. Cacciari and G. P. Salam, *Phys. Lett. B* **641** (2006) 57 [arXiv:hep-ph/0512210].
- [41] S. Alioli, P. Nason, C. Oleari and E. Re, *JHEP* **0904** (2009) 002 [arXiv:0812.0578 [hep-ph]].
- [42] P. Nason, *PoS RADCOR2009* (2010) 018 [arXiv:1001.2747 [hep-ph]].
- [43] V. M. Abazov *et al.* [D0 Collaboration], *Phys. Rev. D* **80** (2009) 053012 [arXiv:0907.4398 [hep-ex]].
- [44] J. Alcaraz *et al.* [ALEPH Collaboration and DELPHI Collaboration and L3 Collaboration and OPAL Collaboration and LEP Electroweak Working Group], arXiv:hep-ex/0612034.
- [45] K. Hagiwara, S. Ishihara, R. Szalapski and D. Zeppenfeld, *Phys. Rev. D* **48** (1993) 2182.
- [46] F. Petriello, *Production of the Higgs and other EW Objects at the LHC*, Talk given at “Physics at the LHC”, Perugia, June 2011.
- [47] K. Hagiwara, R. D. Peccei, D. Zeppenfeld and K. Hikasa, *Nucl. Phys. B* **282** (1987) 253.
- [48] U. Baur and D. Zeppenfeld, *Phys. Lett. B* **201** (1988) 383.
- [49] U. Baur and D. Zeppenfeld, *Nucl. Phys. B* **308** (1988) 127.
- [50] D. Abbaneo *et al.* [ALEPH Collaboration, DELPHI Collaboration, L3 Collaboration, OPAL Collaboration, LEP Electroweak Working Group, SLD Heavy Flavor Group], arXiv:hep-ex/0212036.
- [51] H. Aihara *et al.*, arXiv:hep-ph/9503425.
- [52] L. D’Errico and P. Richardson, arXiv:1106.3939 [hep-ph].
- [53] S. Alioli, P. Nason, C. Oleari and E. Re, *JHEP* **0807** (2008) 060 [arXiv:0805.4802 [hep-ph]].